

Special Issue: Polymers for Microelectronics

Guest Editors: Dr Brian Knapp (Promerus LLC) and
Prof. Paul A. Kohl (Georgia Institute of Technology)

EDITORIAL

Polymers for Microelectronics

B. Knapp and P. A. Kohl, *J. Appl. Polym. Sci.* 2014, DOI: [10.1002/app.41233](https://doi.org/10.1002/app.41233)

REVIEW

Negative differential conductance materials for flexible electronics

A. Nogaret, *J. Appl. Polym. Sci.* 2014, DOI: [10.1002/app.40169](https://doi.org/10.1002/app.40169)

RESEARCH ARTICLES

Generic roll-to-roll compatible method for insolubilizing and stabilizing conjugated active layers based on low energy electron irradiation

M. Helgesen, J. E. Carlé, J. Helt-Hansen, A. Miller, and F. C. Krebs, *J. Appl. Polym. Sci.* 2014, DOI: [10.1002/app.40795](https://doi.org/10.1002/app.40795)

Selective etching of polylactic acid in poly(styrene)-block-poly(D,L)lactide diblock copolymer for nanoscale patterning

C. Cummins, P. Mokarian-Tabari, J. D. Holmes, and M. A. Morris, *J. Appl. Polym. Sci.* 2014, DOI: [10.1002/app.40798](https://doi.org/10.1002/app.40798)

Preparation and dielectric behavior of polyvinylidene fluoride composite filled with modified graphite nanoplatelet

P. Xie, Y. Li, and J. Qiu, *J. Appl. Polym. Sci.* 2014, DOI: [10.1002/app.40229](https://doi.org/10.1002/app.40229)

Design of a nanostructured electromagnetic polyaniline–Keggin iron–clay composite modified electrochemical sensor for the nanomolar detection of ascorbic acid

R. V. Lilly, S. J. Devaki, R. K. Narayanan, and N. K. Sadanandhan, *J. Appl. Polym. Sci.* 2014, DOI: [10.1002/app.40936](https://doi.org/10.1002/app.40936)

Synthesis and characterization of novel phosphorous-silicone-nitrogen flame retardant and evaluation of its flame retardancy for epoxy thermosets

Z.-S. Li, J.-G. Liu, T. Song, D.-X. Shen, and S.-Y. Yang, *J. Appl. Polym. Sci.* 2014, DOI: [10.1002/app.40412](https://doi.org/10.1002/app.40412)

Electrical percolation behavior and electromagnetic shielding effectiveness of polyimide nanocomposites filled with carbon nanofibers

L. Nayak, T. K. Chaki, and D. Khastgir, *J. Appl. Polym. Sci.* 2014, DOI: [10.1002/app.40914](https://doi.org/10.1002/app.40914)

Morphological influence of carbon modifiers on the electromagnetic shielding of their linear low density polyethylene composites

B. S. Villacorta and A. A. Ogale, *J. Appl. Polym. Sci.* 2014, DOI: [10.1002/app.41055](https://doi.org/10.1002/app.41055)

Electrical and EMI shielding characterization of multiwalled carbon nanotube/polystyrene composites

V. K. Sachdev, S. Bhattacharya, K. Patel, S. K. Sharma, N. C. Mehra, and R. P. Tandon, *J. Appl. Polym. Sci.* 2014, DOI: [10.1002/app.40201](https://doi.org/10.1002/app.40201)

Anomalous water absorption by microelectronic encapsulants due to hygrothermal-induced degradation

M. van Soestbergen and A. Mavinkurve, *J. Appl. Polym. Sci.* 2014, DOI: [10.1002/app.41192](https://doi.org/10.1002/app.41192)

Design of cyanate ester/azomethine/ZrO₂ nanocomposites high-k dielectric materials by single step sol-gel approach

M. Ariraman, R. Sasi Kumar and M. Alagar, *J. Appl. Polym. Sci.* 2014, DOI: [10.1002/app.41097](https://doi.org/10.1002/app.41097)

Furan/imide Diels–Alder polymers as dielectric materials

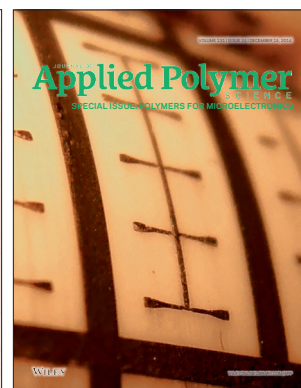
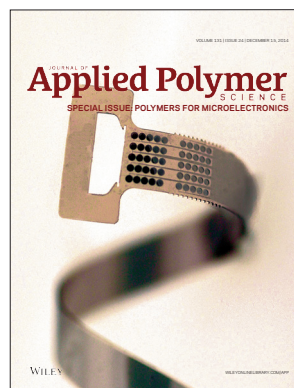
R. G. Lorenzini and G. A. Sotzing, *J. Appl. Polym. Sci.* 2014, DOI: [10.1002/app.40179](https://doi.org/10.1002/app.40179)

High dielectric constant polyimide derived from 5,5'-bis[(4-amino) phenoxy]-2,2'-bipyrimidine

X. Peng, Q. Wu, S. Jiang, M. Hanif, S. Chen, and H. Hou, *J. Appl. Polym. Sci.* 2014, DOI: [10.1002/app.40828](https://doi.org/10.1002/app.40828)

The influence of rigid and flexible monomers on the physical-chemical properties of polyimides

T. F. da Conceição and M. I. Felisberti, *J. Appl. Polym. Sci.* 2014, DOI: [10.1002/app.40351](https://doi.org/10.1002/app.40351)



Special Issue: Polymers for Microelectronics

Guest Editors: Dr Brian Knapp (Promerus LLC) and
Prof. Paul A. Kohl (Georgia Institute of Technology)

Development of polynorbornene as a structural material for microfluidics and flexible BioMEMS

A. E. Hess-Dunning, R. L. Smith, and C. A. Zorman, *J. Appl. Polym. Sci.* 2014, DOI: [10.1002/app.40969](https://doi.org/10.1002/app.40969)

A thin film encapsulation layer fabricated via initiated chemical vapor deposition and atomic layer deposition

B. J. Kim, D. H. Kim, S. Y. Kang, S. D. Ahn, and S. G. Im, *J. Appl. Polym. Sci.* 2014, DOI: [10.1002/app.40974](https://doi.org/10.1002/app.40974)

Surface relief gratings induced by pulsed laser irradiation in low glass-transition temperature azopolysiloxanes

V. Damian, E. Resmerita, I. Stoica, C. Ibanescu, L. Sacarescu, L. Rocha, and N. Hurduc, *J. Appl. Polym. Sci.* 2014, DOI: [10.1002/app.41015](https://doi.org/10.1002/app.41015)

Polymer-based route to ferroelectric lead strontium titanate thin films

M. Benkler, J. Hobmaier, U. Gleißner, A. Medesi, D. Hertkorn, and T. Hanemann, *J. Appl. Polym. Sci.* 2014, DOI: [10.1002/app.40901](https://doi.org/10.1002/app.40901)

The influence of dispersants that contain polyethylene oxide groups on the electrical resistivity of silver paste

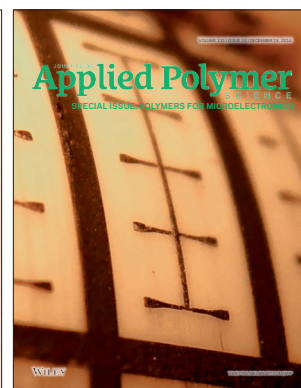
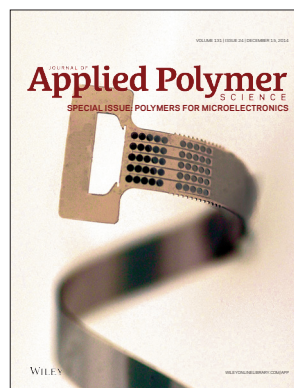
T. H. Chiang, Y.-F. Chen, Y. C. Lin, and E. Y. Chen, *J. Appl. Polym. Sci.* 2014, DOI: [10.1002/app.41183](https://doi.org/10.1002/app.41183)

Quantitative investigation of the adhesion strength between an SU-8 photoresist and a metal substrate by scratch tests

X. Zhang, L. Du, and M. Zhao, *J. Appl. Polym. Sci.* 2014, DOI: [10.1002/app.41108](https://doi.org/10.1002/app.41108)

Thermodynamic and kinetic aspects of defectivity in directed self-assembly of cylinder-forming diblock copolymers in laterally confining thin channels

B. Kim, N. Laachi, K. T. Delaney, M. Carilli, E. J. Kramer, and G. H. Fredrickson, *J. Appl. Polym. Sci.* 2014, DOI: [10.1002/app.40790](https://doi.org/10.1002/app.40790)



Anomalous Water Absorption by Microelectronic Encapsulants due to Hygrothermal-Induced Degradation

Michiel van Soestbergen, Amar Mavinkurve

NXP Semiconductors, Nijmegen, 6534 AE, The Netherlands

Correspondence to: M. van Soestbergen (E-mail: michiel.van.soestbergen@nxp.com)

ABSTRACT: Epoxy molding compounds are widely used as microelectronic encapsulants to protect the electronic circuitry from moisture. Since these compounds are hydrophilic they impose a reliability risk, which is assessed by lifetime tests. The interpretation of these tests is generally based on Fickian absorption. However, this work demonstrates that water absorption by microelectronic encapsulants shows anomalous behavior due to hygrothermal-induced degradation of the material. Namely, experimental data show that the absorption by maiden samples is much slower than subsequent (de)sorption cycles, whereas the solubility depends on the highest water content that was reached in the history of the material. Moreover, at temperatures above glass transition the material might even physically decompose due to water exposure. Comparing these results with common theoretical models for anomalous water absorption shows that the experimental observed anomalies are most likely triggered by internal degradation of the encapsulant, which will impact the reliability assessment of epoxy encapsulated microelectronics. © 2014 Wiley Periodicals, Inc. *J. Appl. Polym. Sci.* **2014**, *131*, 41192.

KEYWORDS: packaging; properties and characterization; thermosets

Received 13 March 2014; accepted 20 June 2014

DOI: 10.1002/app.41192

INTRODUCTION

The majority of microelectronic devices are encapsulated in highly filled epoxy molding compounds, which protect these micro-scale devices from environmental hazards such as moisture and contaminants (see Figure 1). However, these encapsulation materials are slightly hydrophilic since they can absorb up to ~0.6 wt % of water.¹ The absorbed water can have a significant effect on the performance of the encapsulation material since it can (i) alter the mechanical properties of the epoxy, (ii) degrade adhesion between the epoxy and the microelectronic device, (iii) induce mechanical loading due to swelling of the material, or (iv) promote corrosion of the metallization layers on top of the devices.^{2–7} Consequently, the absorption of moisture by epoxy molding compounds is a major concern for the reliability of plastic encapsulated microelectronics.

Microelectronics devices are severely tested to assess their reliability. Reliability tests include exposure of products to high humidity at elevated temperatures, for example, the humidity temperature bias test at 85°C and 85% Relative Humidity (RH) for 1024 h, or the highly accelerated stress test (HAST) at 130°C and 85% RH for 96 h. The results of these tests are translated into operational conditions using (appropriate) acceleration models, which are generally of an empirical nature. Acceleration models that are based on the physicochemical processes underlying reliability require a thorough understanding of the water absorption process.

Because of its simplicity, it is often assumed that water absorption follows Fick's law, that is, water absorption is often described using a mathematically linear set of equations, where transport is driven solely by a concentration gradient, and a clear saturation level is reached within a finite period of time. However, anomalous water absorption has been reported for molding compounds (and epoxy resins in general) in numerous communications.^{8–16} Three different effects were mainly reported, namely; (i) the absence of a clear saturation plateau,^{8–11} (ii) differences in diffusivity during a sorption-desorption-resorption cycle,^{10,12} and (iii) temperature-history dependent diffusion.^{13,17} To describe these anomalies different mathematical models have been previously proposed, which are, for example, based on the free volume concept or chemical bonding of water to polar groups of the polymer.^{6,14,15,18,19} To discriminate between these mathematical models, and consequently use them for performance predictions, experimental data on anomalous water absorption by materials for microelectronics encapsulations are still required.

Previous studies have primarily investigated water absorption under relatively mild conditions; however, absorption under harsh conditions (such as HAST) has had little attention. In order to address this we report a water absorption study on commercially available molding compounds under a wide range of conditions (including HAST), and show that anomalies from a purely Fickian behavior occur. These anomalies are then qualitatively compared with two common theoretical models for

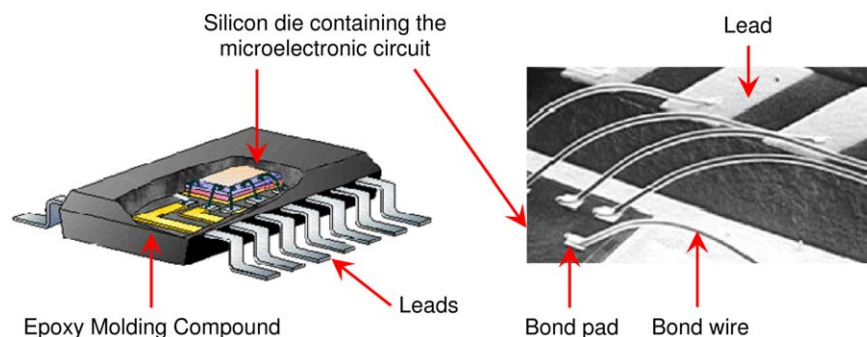


Figure 1. Example of a simple outline package; (a) schematics of a silicon die encapsulated in a molding compound with metal leads, which are used to connect the product to a printed circuit board and (b) electron microscope image of the wires connecting the silicon die to the leads. [Color figure can be viewed in the online issue, which is available at wileyonlinelibrary.com.]

anomalous diffusion. Furthermore, we show that at the most severe conditions at which microelectronics are stressed during reliability tests a clear degradation of the epoxy material occurs. An effect that, until now, has been largely overlooked by the microelectronic packaging community.

This contribution is organized as follows; first, we will restate Fick's theory and discuss models for anomalous water absorption, next we will describe our experimental approach, and present the experimental results in the following section, whereas finally we will discuss our results in view of the performance of epoxy molding compounds as microelectronic encapsulation materials.

THEORY

In this section, we will recapitulate Fick's theory for diffusion, and outline some of the major approaches to model anomalous behavior.

Linear Theory

Fick's law states that water diffuses from a region of high concentration to a region of low concentration at a flux equal to,

$$\mathbf{J} = -D \nabla C, \quad (1)$$

where D is the diffusion coefficient of water in the respective medium and ∇C is the gradient in concentration. Combining eq. (1) with a mass balance and assuming a uniform diffusion coefficient yields,

$$\dot{C} = D \Delta C, \quad (2)$$

which is often referred to as Fick's second law of diffusion, where \dot{C} and ΔC denote the time derivative and the Laplacian of the concentration, respectively.

According to eq. (2) the mass of water in a three dimensional rectangular specimen becomes,¹⁴

$$M = (1-g)(M_\infty - M_i) + M_i$$

$$g = \frac{516}{\pi^6} \sum_{k,l,m=0}^{\infty} \frac{\exp \left[-D\pi^2 \left(\left(\frac{2k+1}{x_0} \right)^2 + \left(\frac{2l+1}{y_0} \right)^2 + \left(\frac{2m+1}{z_0} \right)^2 \right) t \right]}{(2k+1)^2 (2l+1)^2 (2m+1)^2} \quad (3)$$

where t is the time, x_0 , y_0 and z_0 are the specimen dimensions, M_∞ is the final mass of the water in the sample at equilibrium

(which e.g., equals the saturation level during sorption or zero during desorption), and M_i is the initial mass of the water in the sample.

In conjunction with Fick's theory, the water concentration inside the material (or likewise the mass of water in the material) at saturation, C_{sat} , can be determined from Henry's law,

$$C_{sat} = S P_v, \quad (4)$$

where S is the solubility coefficient and P_v the water vapor pressure surrounding the material. In this work, it is assumed that the solubility coefficient obeys an Arrhenius behavior,

$$S = S_0 \exp \left(-\frac{E_a}{k_B T} \right), \quad (5)$$

where S_0 is a prefactor, E_a is the activation energy, k_B is Boltzmann's constant, and T is the temperature.

Furthermore, we assume that the overall saturation concentration in the material depends linearly on the amount of filler particles in the material according to,

$$C_{sat} = C_{sat,pol}(1-\phi) + C_{sat,fil} \phi, \quad (6)$$

where ϕ is the weight fraction of filler particles, and subscript "sat" and "fil" indicate the saturation concentration of the polymer and filler phase, respectively. Note, that the filler particles are generally fused silica, which cannot absorb significant amounts of water. However, deviations from the ideal mixing law might occur.²⁰ It is, for example, possible that water either locally adsorbs onto the filler surface, or resides at a higher concentration at the filler-epoxy interface compared to the bulk due to local distortions of the polymer chains induced by the presence of the filler particles. In both cases, this will be macroscopically observed as a nonzero "saturation" concentration for the filler particles.

Models for Anomalous Absorption

Experiments on water sorption by polymers have revealed several effects that are not well captured by the linear Fickian theory (see the introduction section). In the literature, several mathematical models have been proposed to describe these effects.

A straightforward, and mathematical appealing, extension is to combine two Fickian diffusion models, using the co-called "dual

stage" model,^{11,21–25} where the total mass of water in the specimen is given by

$$M_{tot} = M_{fast} + M_{slow}, \quad (7)$$

with M_{fast} and M_{slow} according to eq. (3) with each an own diffusion coefficient and saturation limit. Here, water is considered to be present in two completely independent phases; the first phase (M_{fast}) represents fast transport, for example, via macrovoids, whereas the second phase (M_{slow}) represent slow absorption, for example, due to diffusion into microcavities.

A similar approach to the dual stage model is to consider that water can be present in either a free phase, or can be bound to polar groups of the polymer.^{18,26} The transition from free water to bound water can, for example, be described by Langmuir adsorption.²⁷ In one dimension the water uptake is then described by²⁸

$$M = M_{\infty} \left\{ 1 - \frac{\beta}{\alpha + \beta} \exp(-\alpha t) - \frac{\alpha}{\alpha + \beta} \frac{8}{\pi^2} \sum_{n=0}^{\infty} \frac{1}{(2n+1)^2} \exp\left(-\pi^2 [2n+1]^2 \frac{D}{z_0^2} t\right) \right\}, \quad (8)$$

where α is the probability of free water molecules to become bound, and β is the probability of bound water to become free. Note that eq. (8) is derived under the assumption that $\alpha, \beta \ll D\pi^2/h^2$.

A completely different approach is to consider the viscoelasticity of the material. Polymer materials are viscoelastic by nature and exhibit creep under mechanical pressure. As a result any internal induced stress due to swelling might relax, which enables an increase in water absorption. Several models based on creep relaxation have been proposed in literature.^{29–31} Moreover, the concept of "hidden" thermodynamic state variables, ξ_i , has been proposed to determine the temperature-history dependence of diffusion. Here, the volume fraction of microvoids, which may form in the material under the combined action of temperature and humidity, can be used as the hidden internal state variable.¹³ In these models, the diffusion coefficient and the solubility take the form, $D = D(\xi_i)$, and $C = C(\xi_i)$, respectively. In this case, the solution to the diffusion equation, that is, eq. (2), requires a mathematical description of the dependence of the diffusion coefficient and solubility on these hidden state variables. Such a description is, however, beyond the scope of this work. Although the above-mentioned approaches all appear promising, a unified model that is widely accepted is still lacking.

EXPERIMENTAL

All experiments were performed on commercially available epoxy molding compounds that are used by the microelectronics industry. We report data on the saturation level of both *o*-cresol novolac (OCN) as well as biphenyl (BPH) based molding compounds. However, the majority of experimental data is on a low molecular BPH based molding compound, which contains ~89 wt % of fused silica filler particles. The glass transition temperature of this material is ~110°C under dry conditions.

Samples were fabricated by injecting the epoxy compound into a mold at a temperature of 180°C. The samples were pre-cured

in the mold for 90 s and postcured at 175°C for 4 h. Note that omitting the post mold cure will lower the barrier properties of the encapsulant.³² This postmold cure also ensured that the samples were dry at the beginning of the water uptake experiments. The final sample dimensions were 49.5 × 9.5 × 2 mm.

The samples were either exposed to a water bath or a humid environment. The water bath was obtained by pouring ~100 mL of demi-water into a glass beaker in which the samples were immersed. The beakers were subsequently covered with aluminum foil to prevent evaporation of water. Finally, the beakers were placed inside an oven at the designated temperature. The water bath experiments above 100°C required pressure vessels. Therefore, nonstirred pressure vessels from the Parr Instrument Company, which consist of a 100 mL stainless steel housing with a PTFE lining, were used for these experiments. For the experiments, at controlled humidity a climate chamber has been used (Vötsch VC4018). Here, the samples were placed on a mesh of fine metal wires to ensure full exposure of the sample to the humid environment.

At several time intervals, the samples were removed from either the water bath or the climate chamber and weighed on a balance. The samples coming from the water bath were first wiped with a paper tissue to remove any surface water. Prior to recording the mass, the samples were equilibrated with their new environment for some minutes to obtain a stable reading from the balance. The samples were then placed back under the experimental conditions, except for the experiments that were performed under HAST conditions, since here it takes too long to (de)pressurize the chamber.

RESULTS AND DISCUSSION

In this section, we present results for the water uptake of several molding compounds. First, an analysis based on Fickian diffusion will be presented. Next, we show the absence of a clear saturation level. Subsequently, the history dependence of water absorption will be discussed. Finally, we will show data for water absorption under extreme conditions at temperatures above glass transition.

Fickian Diffusion

As an example of Fickian diffusion the characteristic water uptake for two different types of molding compounds at 30°C and 60% RH is presented in Figure 2(a,b). Under these experimental conditions, the materials behave approximately Fickian, with an initial water uptake that increases linearly as a function of \sqrt{t} , and which levels off at an apparent saturation level. This is illustrated by the fit of this data to the Fickian theory of eq. (3), which is represented by the dashed line. The fitted values for these lines are $D = 2.53 \times 10^{-13} \text{ m}^2/\text{s}$ and $M_{\infty} = 0.285 \text{ wt } \%$ for the OCN compound of Figure 2(a), and $D = 3.40 \times 10^{-13} \text{ m}^2/\text{s}$ and $M_{\infty} = 0.088 \text{ wt } \%$ for the BPH compound of Figure 2(b). The high saturation level of the OCN compound compared with the BPH compound is due to the lower filler content of the former.

The apparent saturation level for various compounds at $T = 85^\circ\text{C}$ and $\text{RH} = 85\%$ as a function of the amount of fillers is given in Figure 2(c). The saturation level decreases with increasing filler amount since the fillers take out volume in the

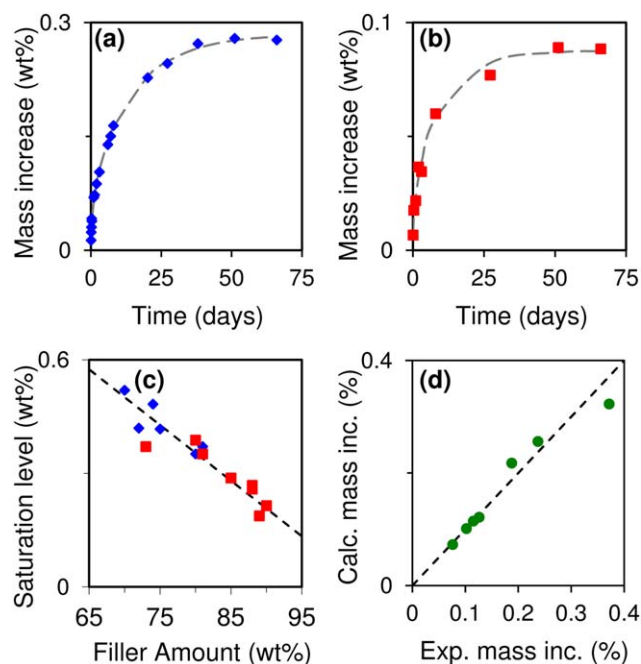


Figure 2. Apparent Fickian diffusion; (a) mass increase for an OCN compound at 30°C and 60% RH, the dashed line represent eq. (3); (b) same as (a) for a BPH compound; (c) moisture saturation level at 85°C and 85% RH as a function of the filler amount, the diamonds and squares represent OCN and BPH compounds, respectively, the dashed lines indicates eq. (6); (d) calculated mass increase according to eq. (5) as a function of the experimental mass increase for a BPH compound. [Color figure can be viewed in the online issue, which is available at wileyonlinelibrary.com.]

material for the water to reside. The overall trend for several types of molding compounds is remarkable; the saturation level decreases approximately linear as a function of the filler amount according to eq. (4) with $C_{\text{sat,pol}} = 1.53 \text{ wt } \%$ and $C_{\text{sat,fil}} = 0.06 \text{ wt } \%$. This indicates that the filler particles cannot be simply treated as “dead” volume, which takes out space for the water to reside, but rather they also slightly promote water absorption as discussed in the theory section.

In Figure 2(d), the calculated saturation level according to Henry’s law, that is, eq. (5), for the BPH compound containing 89 wt % of fillers is given as a function of the experimentally observed saturation level. Note that in case a clear saturation level was absent (to be discussed below) we used an estimated saturation level according to Fickian theory. Figure 2(d) shows that the experimental data can be fairly well described by Henry’s law over the whole range of experimental conditions with temperatures between 30 and 130°C at a humidity ranging from 60 to 100% RH. The fit parameters are $S_0 = 1.52 \times 10^{-10} \text{ wt } \%/ \text{Pa}$, and $E_a = -0.317 \text{ eV } (-30.6 \text{ kJ/mol})$. Our value for E_a is comparable to that of common polymers such as polyethylene terephthalate, -28 kJ/mol , and poly(methyl methacrylate), -37 kJ/mol .³³ Merdas et al. suggested that this activation energy equals the heat of dissolution.³³ Consequently, the activation energy found in this work indicates that the water absorption is exothermic, which indicates a relatively high number of hydrophilic sites within the material.³³ Indeed, a FTIR study by Li

et al. on a Novolac epoxy showed strong binding between the water and hydrophilic groups within the material.³⁴ Finally, note that E_a gives the temperature dependence of the solubility coefficient; the temperature dependence of the saturation concentration includes the temperature dependence of the water vapor pressure, which can be approximated by an Arrhenius equation with an activation energy of 43 kJ/mol.³³

Absence of a Saturation Level

In the previous subsection, it is reported that the absorption curves under mild conditions (30°C and 60% RH) follow the Fickian theory. We will now show that under more severe conditions anomalies might occur. In Figure 3, the evolution of the mass increase of the BPH molding compound immersed in water at 80°C is given. The initial data points can be fitted to the Fickian theory of eq. (3) with a saturation level of 0.223 wt %. Henry’s law with the parameters given in the previous subsection predicts a saturation level of 0.242 wt %, which is fairly comparable. However, from ~25 days onward deviations from the Fickian prediction start to occur. It is observed that the mass increase does not level off any further, but starts to increase linearly as a function of time. This increase continues up to 130 days, with a slope of $\sim 0.003 \text{ wt } \%/ \text{day}$. At the end of the experiment, the water content in the sample was more than twice the saturation level as predicted by Henry’s law.

History Dependence

In Figure 4, the results for a sorption-desorption-resorption cycle are given. The cycle was performed by first immersing samples in a water bath at $T = 80^\circ\text{C}$ until they reach their apparent saturation level (as discussed in section “Absence of a saturation level”). After this initial sorption period, the samples were taken from their water bath and were air dried in an oven at $T = 80^\circ\text{C}$. This desorption period continued until the samples retained their initial mass. Subsequently, the samples were

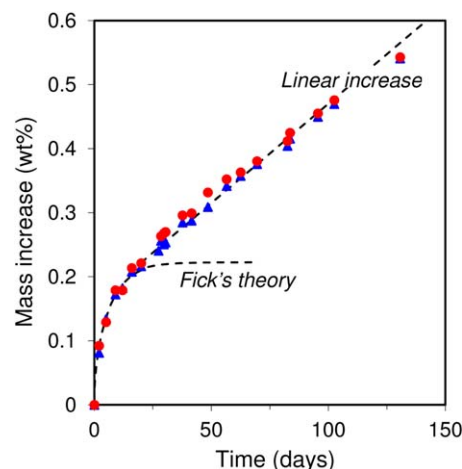


Figure 3. Mass increase of a BPH molding compound during prolonged absorption in liquid water at $T = 80^\circ\text{C}$. The symbols indicate the experimental data of each set, and the dashed lines indicate Fickian absorption ($D_{\text{abs}} = 5.23 \times 10^{-11} \text{ m}^2/\text{s}$, $C_{\text{sat}} = 0.222\%$), and a linear increase, respectively. [Color figure can be viewed in the online issue, which is available at wileyonlinelibrary.com.]

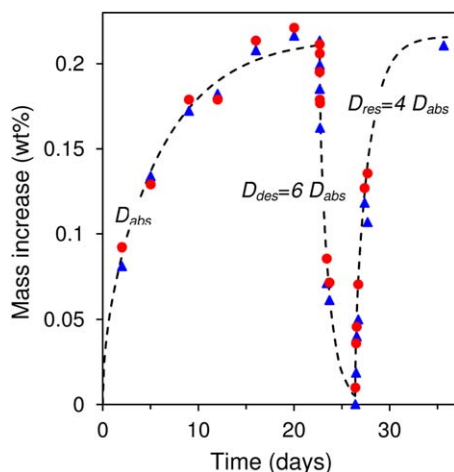


Figure 4. Mass increase of a BPH molding compound during a sorption-desorption-resorption cycle; (re)sorption in liquid water at $T = 80^\circ\text{C}$, desorption in air at $T = 80^\circ\text{C}$. The symbols indicate the experimental data of each set, and the dashed line represents the Fickian prediction with $D_{\text{abs}} = 5.23 \times 10^{-11} \text{ m}^2/\text{s}$ and $C_{\text{sat}} = 0.222\%$. [Color figure can be viewed in the online issue, which is available at wileyonlinelibrary.com.]

again immersed in a water bath at $T = 80^\circ\text{C}$ to start the resorption period.

The initial sorption period is well described by eq. (3) with a diffusion coefficient equal to $D_{\text{abs}} = 5.23 \times 10^{-11} \text{ m}^2/\text{s}$. The subsequent desorption, however, can only be described by taking a six times higher diffusion coefficient, whereas the final resorption cycle is described by a four times higher coefficient than the diffusion coefficient for the initial absorption step. This displays the fact the water absorption rate is clearly history dependent.

Next, we will show another effect of the hygrothermal history of the sample on its water absorption. We first expose samples to

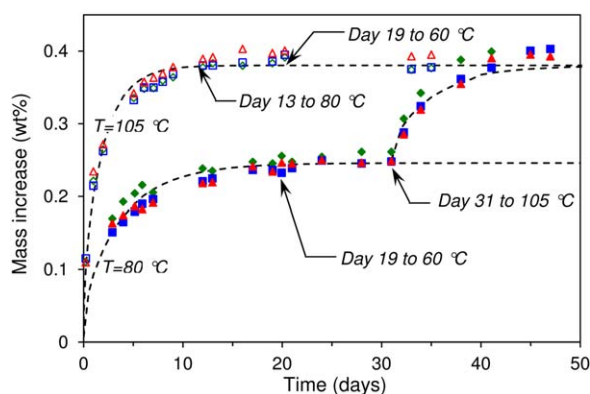


Figure 5. History dependence of moisture absorption by BPH molding compound. One data set (open symbols) represent samples that were initially exposed to liquid water at $T = 105^\circ\text{C}$, after which they were transferred to a 80°C bath at day 13 and a 60°C bath at day 19. The other data set (filled symbols) represent a similar cycle; starting from 80°C to 60°C at day 19, and then 105°C at day 31. The dashed lines represent fits to Fick's theory. [Color figure can be viewed in the online issue, which is available at wileyonlinelibrary.com.]

a water bath at $T = 105^\circ\text{C}$ until an apparent saturation level is reached. The corresponding absorption curve shows a near Fickian behavior as indicated in Figure 5. After the apparent saturation level was reached, the samples were taken from the water bath at $T = 105^\circ\text{C}$ and placed in a water bath at $T = 60^\circ\text{C}$. Henry's law now predicts a decrease in water absorption by the samples. However, such a loss of water was not observed experimentally as the mass increase remains at the apparent saturation level that was reached at $T = 105^\circ\text{C}$. This counter intuitive behavior is further illustrated by samples that were first exposed to a water bath at $T = 80^\circ\text{C}$ until 19 days, after which they were placed in water bath at $T = 60^\circ\text{C}$. Again, no decrease in the water content was observed (see Figure 5). However, the samples do show additional water absorption in response to a subsequent exposure to a water bath at $T = 105^\circ\text{C}$ from day 31 onward. This water absorption increases until the same apparent saturation level was reached as for the samples that were first exposed to water at $T = 105^\circ\text{C}$.

Comparison with Theoretical Models

In this section, we will compare the anomalous absorption reported in the previous subsections with the theoretical models of section "Models for anomalous absorption." In Figure 6(a), it is shown that the absence of a plateau level can be accurately described by the Langmuir model, that is, eq. (8). Here, the following constants are used: $D = 10^{-12} \times \text{m}^2/\text{s}$, $\alpha = 2.5 \times 10^{-7} \text{ 1/s}$, $\beta = 3 \times 10^{-8} \text{ 1/s}$, and $1.48 \text{ wt } \%$, which represent a slow binding of water to the polymer up till a water content of $1.48 \text{ wt } \%$ is reached. Note that such a plateau level was not observed by Bao et al. as they did not find an equilibrium plateau for a bismaleimide resin after exposure for a year in a water bath.¹¹ The results according to eq. (8) show a clear linear behavior after the initial absorption phase, which fits the experimental data well. For the dual stage model, that is, eq. (7), this clear linear trend is not observed as the line is slightly concave at prolonged times. The parameters used for the dual stage model are: $D_{\text{fast}} = 2.13 \times 10^{-11} \text{ m}^2/\text{s}$, $D_{\text{slow}} = 3.16 \times 10^{-14} \text{ m}^2/\text{s}$, $M_{\text{fast}} = 0.03 \text{ wt } \%$, and $M_{\text{slow}} = 1.22 \text{ wt } \%$, which represent a fast, but slight, initial absorption, followed by a much slower absorption step leading to the majority of water in the sample.

Although both theories predict the absence of a plateau level rather well, they cannot describe the sorption/desorption/resorption behavior of Figure 4 using one consistent set of input parameters as shown in Figure 6(b). Here, the same input parameters as for Figure 6(a) were used to describe the complete cycle. Fan et al. obtained a similar result for a sorption/desorption cycle using the dual stage model, which could only be used to describe their experimental data by adjusting the diffusion coefficients for the subsequent desorption step.³⁵

The adjustment of the diffusion coefficient indicates a transformation of the material. Apicella et al. used an approach based on the formation of microvoids as the internal state variable to explain the temperature-history dependence of diffusion.¹³ These microvoids form irreversibly under the combined action of temperature and humidity, and are believed to control the absorption of water by the material. They state that the solubility of the material consist of two parts; (i) water absorbed by

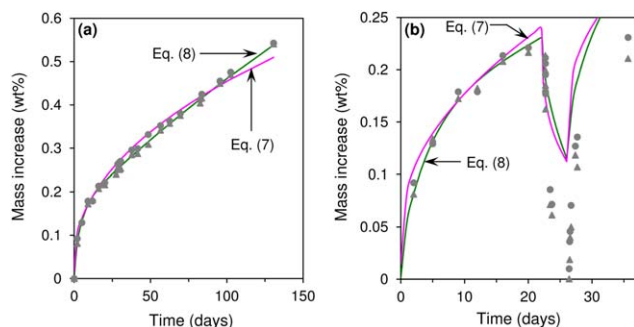


Figure 6. Comparison between the theoretical models for anomalous water absorption and the experimental data of (a) Figure 3 and (b) Figure 4. The lines correspond to the dual stage, eq. (7), and the Lanqmuir, eq. (8), model, whereas the symbols indicate the experimental data. [Color figure can be viewed in the online issue, which is available at wileyonlinelibrary.com.]

the dense polymer fraction, and (ii) water present in microvoids. The content of microvoids in the material can depend on both time and the hydrothermal history of the material (e.g., the highest achieved water concentration in its history). Therefore, this hydrothermal-induced degradation of the material can also explain the history dependence of Figure 5.

Absorption Above Glass Transition

In this section, results are presented for water absorption at a temperature of 130°C, which is well above the glass transition temperature of the BPH molding compound (the glass transition temperature will even decrease due to the absorbed water). At this temperature, samples were exposed to both a water bath, and 85% RH in a humidity chamber. This latter condition equals the HAST condition, which is used for accelerated reliability tests of microelectronic products.

The results for the water bath show an increase of mass over the first few days, as expected. Then, a counter intuitive result is obtained: namely, the mass starts to decrease, as shown in Figure 7(a). This decrease is not just by a small amount, but drastically, to values even below the initial dry weight. This decrease continued up to even 10 wt % of the initial dry weight after a prolonged

exposure of 100 days [not shown in Figure 7(a)]. This mass decrease indicates that the samples are losing material, which is induced by the absorbed water. Analysis of the water in which the samples were immersed showed that the weight loss is almost completely due to the removal of the silica filler particles. The silicon/carbon mass ratio in the water ranged from 30/1 to 50/1, where the silicon represents the fillers and the carbon any dissolved epoxy material. Apparently, the absorbed water breaks the bond between fillers and the polymer chain, after which the filler particles leach out into the water bath. Consequently, the results of Figure 7(a) represent a severe form of hydrothermal-induced degradation.

Experiments at 85% RH were performed to check if mass loss is also observed when no pathway for filler particle removal is present. After exposing the samples to 85% RH at $T = 130^\circ\text{C}$ they were removed from the humidity chamber and their mass increase was determined. Subsequently, the samples were placed in a water bath at $T = 80^\circ\text{C}$ to check if any filler particles leach out due the high temperature exposure in the humidity chamber. The results of these experiments showed that with increasing time at 85% RH at $T = 130^\circ\text{C}$ the mass of the sample increases, but no decrease was observed at prolonged time [see Figure 7(b)]. Furthermore, after exposure to this condition (even after only 1 day) the mass increase at 80°C in the subsequent water bath is well above the maximum absorption level corresponding to that condition. This implies that if the sample would not have been pretreated at higher temperature its mass increase equals ~ 0.22 wt % as shown in Figure 3. This behavior again shows the thermal hydrothermal history-effect as discussed in the previous section, which can be contributed to hydrothermal-induced degradation at this (HAST) condition.

The results presented in Figure 7(a,b) show that exposure of the molding compound to a water bath at high temperatures ($T = 130^\circ\text{C}$) triggers damage of the compound that does not occur under humid conditions at 85% RH. Consequently, immersion experiments at high temperatures cannot be used to accelerate the effect of water vapor diffusion since different mechanisms are involved in both cases.²⁸

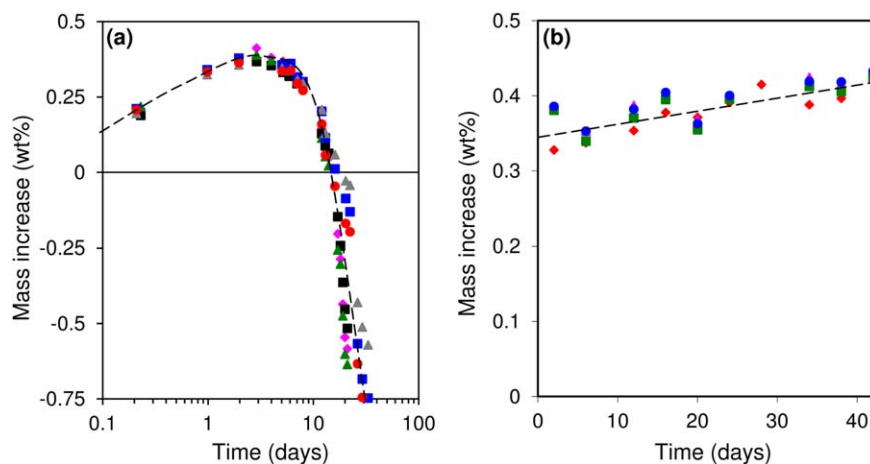


Figure 7. Mass increase of BPH molding compound above glass transition at 130°C; (a) for samples immersed in a water bath, and (b) for samples exposed to 85% RH. The dashed lines are guides-to-the-eye. [Color figure can be viewed in the online issue, which is available at wileyonlinelibrary.com.]

CONCLUSIONS

The results presented in this work confirm other work published in the literature regarding a few facts; water uptake by epoxy molding compounds does not always follow Fick's law. Water absorption depends on the hygrothermal history of the sample due to hygrothermal-induced degradation of the encapsulant. This will be most pronounced during temperature-humidity cycles with a varying magnitude, which will occur during the operational life of products. Fickian absorption predicts that the water content in the material follows the magnitude of this cycle, whereas the data reported here suggest that the highest magnitude of the cycle should be considered instead. Furthermore, we have shown that water absorption at high RH and high temperatures for an extensive period of time might increase to a level that is much higher than predicted by Henry's law. These aspects are important to consider for the mission profile of microelectronic products.

The above-mentioned severe conditions are not likely to occur in the field. However, package-based reliability assessments for moisture-related failures are usually performed under extreme conditions, where such anomalous behavior will be seen. Temperatures above the glass transition (as might be encountered during the popular HAST reliability test) might lead to unrealistic acceleration models as well, since above glass transition the absorption mechanism might be different than at operating conditions. Hence, it is not trivial to translate the behavior of the package during a reliability assessment to what would happen in the actual application. Consequently, an accelerated test like HAST or PPOT (Pressure Pot, 121°C/100%RH) will usually "overstress" the device. If no failures are observed it will indicate a certain robustness margin. However, if failures do occur, it is essential to perform an assessment that takes this anomalous moisture behavior into account.

The trend of decreasing thickness of handheld devices, as well as their increased functionality, leads to thinner and smaller microelectronic products, which also leads to a reduction of the layer thickness of the epoxy molding compound barrier for products that are exposed to (humid) outdoor environments. Consequently, in the reliability assessment of these products anomalous absorption of moisture needs to be taken into account when using standard reliability assessments to make lifetime predictions.

REFERENCES

1. Ardebili, H.; Wong, E. H.; Pecht, M. *IEEE Trans. Comp. Pack. Tech.* **2003**, *26*, 206.
2. Wong, E. H.; Koh, S. W.; Lee, K. H.; Rajoo, R. *IEEE Trans. Comp. Pack. Tech.* **2002**, *25*, 223.
3. van Gils, M. A. J.; Habets, P. J. J. H. A.; Zhang, G. Q.; van Driel, W. D.; Schreurs, P. J. G. *Microelectron. Reliab* **2004**, *44*, 1317.
4. van Soestbergen, M.; Mavinkurve, A.; Rongen, R. T. H.; Jansen, K. M. B.; Ernst, L. J.; Zhang, G. Q. *Electrochim. Acta* **2010**, *55*, 5459.
5. Shirangi, M. H.; Michel, B. In Mechanism of Moisture Diffusion, Hygroscopic Swelling, and Adhesion Degradation in Epoxy Molding Compounds in Moisture Sensitivity of Plastic Packages of IC Devices; Fan, X. J., Suhir, E., Eds.; **2010**; p 29.
6. Ardebili, H.; Hillman, C.; Natishan, M. A. E.; McCluskey, P.; Pecht, M. G. *IEEE Trans. Comp. Pack. Tech.* **2002**, *25*, 132.
7. Walter, H.; Bauer, J.; Braun, T.; Hölck, O.; Wunderle, B.; Wittler, O. In Proceedings of the International Conference on Thermal Mechanical and Multiphysics Simulations and Experiments in Microelectronic and Micro-Systems; Cascais, Portugal, Institute of Electrical and Electronics Engineers (IEEE): New York, **2012**.
8. Vanlandingham, M. R.; Eduljee, R. F.; Gillespie, J. W. J. *Appl. Polym. Sci.* **1999**, *71*, 787.
9. Wong, E. H.; Rajoo, R. *Microelectron. Reliab.* **2003**, *43*, 2087.
10. Wong, T. C.; Broutman, L. J. *Polym. Eng. Sci.* **1985**, *25*, 521.
11. Bao, L.; Yee, A. F.; Lee, C. Y. *Polymer* **2001**, *42*, 7327.
12. Lin, Y. C.; Chen, X. *Polymer* **2005**, *46*, 11994.
13. Apicella, A.; Nicolais, L.; Astarita, G.; Drioli, E. *Polymer* **1979**, *20*, 1143.
14. Crank, J. *Mathematics of Diffusion*; Clarendon Press, Oxford **1975**.
15. Glaskova, T. I.; Guedes, R. M.; Morais, J. J.; Aniskevich, A. N. *Mech. Comp. Mater.* **2007**, *43*, 377.
16. Fan, X. J.; Lee, S. W. R.; Han, Q. *Microelectron. Reliab.* **2009**, *49*, 861.
17. El-Sa'ad, L.; Darby, M. I.; Yates, B. J. *Mater. Sci.* **1990**, *25*, 3577.
18. Soles, C. L.; Yee, A. F. *J. Polym. Sci. Part B: Polym. Phys.* **2000**, *38*, 792.
19. El Yagoubi, J.; Lubineau, G.; Roger, E.; Verdu, J. *Polymer* **2012**, *53*, 5582.
20. Prolongo, S. G.; Gude, M. R.; Ureña, A. *Compos. A* **2012**, *43*, 2169.
21. Placette, M. D.; Fan, X. J.; Zhao, J.-H.; Edwards, D. *Microelectron. Reliab.* **2012**, *52*, 1401.
22. Barclay, M.; Satterfield, Benziger, J. B. *J. Phys. Chem. B* **2008**, *112*, 3693.
23. Shirangi, H.; Auersperg, J.; Koyuncu, M.; Walter, H.; Müller, W. H.; Michel, B. In Proceedings of the International Conference on Thermal Mechanical and Multiphysics Simulations and Experiments in Microelectronic and Micro-Systems, Freiburg, Germany, Institute of Electrical and Electronics Engineers (IEEE): New York, **2008**, p 1.
24. Fan, X. J.; Nagaraj, V. In Proceedings of the Electronic Components and Technology Conference, San Diego, CA, Institute of Electrical and Electronics Engineers (IEEE): New York, **2012**, p 1190.
25. Yang, S.; Liu, H. In Proceedings on International Symposium Advanced Packaging Materials, Xiamen, People's Republic of China, **2011**, Institute of Electrical and Electronics Engineers (IEEE): New York, p 336.
26. Lee, M. C.; Peppas, N. A. *Prog. Polym. Sci.* **1993**, *18*, 947.

27. Carter, H. G.; Kibler, K. G. *J. Compos. Mater.* **1978**, *12*, 118.
28. Bonniau, P.; Bunsell, A. R. *J. Compos. Mater.* **1981**, *15*, 272.
29. Liu, H.; Li, J.; Hu, Y. *Fluid Phase Equilib.* **1999**, *158-160*, 1035.
30. Neogi, P. *AIChE J.* **2004**, *29*, 829.
31. Neogi, P. *AIChE J.* **2004**, *29*, 833.
32. Belton, D. J.; Sullivan, E. A.; Molter, M. J. *ACS Symp. Ser.* **1989**, *497*, 186.
33. Merdas, I.; ThomINETTE, F.; Tcharkhtchi, A.; Verdu, J. *Compos. Sci. Technol.* **2002**, *62*, 487.
34. Li, L.; Zhang, S. Y.; Chen, Y. H.; Liu, M. J.; Ding, Y. F.; Luo, X. W.; Pu, Z.; Zhou, W. F.; Li, S. *Chem. Mater.* **2005**, *17*, 839.
35. Fan, X. J.; Nagaraj, V. In Proceedings of the International Conference on Thermal Mechanical and Multiphysics Simulations and Experiments in Microelectronic and Micro-Systems, Cascais, Portugal, Institute of Electrical and Electronics Engineers (IEEE): New York, **2012**.